Study of laser-induced forward transfer dynamics of a conductive silver ink

Author: Ferran Bonet Isidro
Advisor: Pere Serra Coromina
Departament de Física Aplicada, Facultat de Física, Universitat de Barcelona, Diagonal 645, 08028 Barcelona, Spain.*

Abstract: A study of laser-induced forward transfer technique using a low viscosity silver nanoparticle ink is performed. Images of the process were obtained with sub-microsecond resolution that reveal different transfer dynamics depending on the fluence employed. After the laser pulse interacts with the source material, an ink jet that advances at constant speed that depends on the fluence is observed. Further analysis of the printed droplets with an optical microscope shows an optimal fluence range for which semi-spherical droplets are obtained.

I. INTRODUCTION

There is a wide variety of techniques available to deposit small amounts of material on an acceptor substrate. One of them is inkjet printing, a low-cost technique capable of printing electronic devices [1]. This method involves the use of a nozzle to deposit a droplet of ink on a substrate. However, it has drawbacks, including limitations related to the ink viscosity and dried ink that can cause the clogging of the nozzle [2]. These factors limit the range of materials that can be printed with inkjet printing. An alternative direct-writing family of techniques is laser direct-write addition (LDW+). This approach allows the deposition of material without the constraints of the nozzle and grants the preservation of the properties of the material to be deposited. With this technique, it is also possible to print an extensive diversity of materials useful in fields like microelectronics, power generating systems and biology [3].

A particular LDW+ technique is laser-induced forward transfer or LIFT. In LIFT, a transparent donor substrate contains a thin film of the material that is to be transferred to the acceptor substrate. Both substrates are placed close to each other and a laser pulse is focused on the donor film. The laser heats a fraction of the material, creating a sudden pressure increase and vaporizing it. Then, the vapor projects the donor material towards the acceptor substrate where it is deposited [3, 4]. Controlling the incident laser energy, it is possible to obtain micrometric resolution in the deposited material [3].

LIFT can be applied to both solid and liquid phase materials [3, 4]. In liquid-phase LIFT it is possible to use inkjet printing conductive inks containing the material wanted to print. In this alternative approach to LIFT a vapor bubble is created when the laser interacts with a small fraction of the source material and this gives rise to a jet that propels the remaining material towards the acceptor substrate [3, 4]. The jet formation is shown in Fig.1. A dynamic release layer (DRL), usually a metal, can be placed between the transparent substrate and the source. This DRL absorbs the energy of the laser instead of the source material. The process is similar to the one explained previously. The DRL minimizes the effects the laser has on the source material such as the increase of temperature or induced phase transitions [3]. The different process dynamics with and without DRL has been studied [5]. In the present work, however, a DRL will not be employed.

The dynamics of the transfer process has already been examined in a variety of papers [6-9] pointing out the parameters that affect the process; for instance, the laser fluence and the laser beam diameter. In these works a mixture of water and glycerol of 50 % (v/v) was the source film while here a nanoparticle silver ink will be used.

In this work the transfer process of micrometric droplets will be examined. Images of the whole transfer process and the resulting deposited droplets will be taken with different laser pulse energies and they will be analysed to better understand the whole operation.

II. EXPERIMENTAL SETUP

To carry out the experiment, a Nd:YAG pulsed laser with a pulse length of 10 ns, a repetition rate of 10 Hz and a wavelength of 355 nm was used. The laser was guided into a Q-Switch containing a quartz crystal that, when oscillating, acts as a diffraction grating. With a semi-transparent mirror, 50 % of the laser was sent towards an energy detector while the remaining fraction was guided through mirrors to a microscope objective with a magnification of 15x specifically prepared to operate with a wavelength of 355 nm. The microscope ensured that the laser was focused onto the sample placed below it. A LED illuminated the sample and the images were taken with a CCD camera. The activation of the LED, the arrival of the laser to the sample and the capturing of the image were synchronized so the exact time wanted to take the image could be chosen to achieve images at different delays respect to the laser pulse and therefore at different stages of the transfer process. The exposure time of the CCD could also be varied.

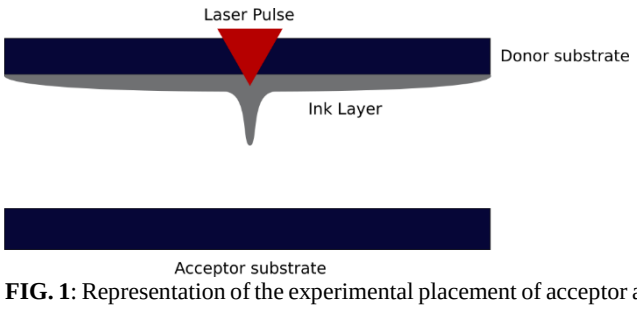

FIG. 1: Representation of the experimental placement of acceptor and donor substrate, the laser focusing and the ink layer.

The transferred material was a silver nanoparticle dispersion ink from Sigma Aldrich (ref.736481). This

* Electronic address: ferran.bonet95@gmail.com

conductive ink has its applications in the world of electronics. Its particle size was smaller than 50 nm, with a surface tension of 0.03-0.05 N/m, a viscosity of 8-10 mPa·s, a solid content of about 30-35 wt. % and a density 1.45 g/mL. The ink was spread on the donor substrate, a glass microscope slide of 25x75 mm^2, through a blade coater. The average ink film had a mass of 36 mg and a thickness of 15 μm. An identical microscope slide was used as an acceptor substrate, it was placed 1.25 mm below the donor substrate, that had previously been covered with the ink. The sample was then turned upside down and set below the microscope as seen in Fig.1.

III. RESULTS AND DISCUSSION

The goal of section A is the characterization of a droplet array, wherein each row of the array was printed with a different laser energy. The purpose of section B is the experimental measurement of the laser beam diameter. Lastly in section C the dynamics of the deposition process is studied.

A. ANALYSIS OF A DROPLET ARRAY

In this section the objective was to print a 5x5 array of droplets at different laser pulse energies ranging from 0.1 μJ to 5 μJ and to analyse its features once they had dried employing an optical microscope (Carl Zeiss, model AX10 Imager.A1). The same setup explained in section II was used with the imaging system turned off. The results are presented in Fig.2.

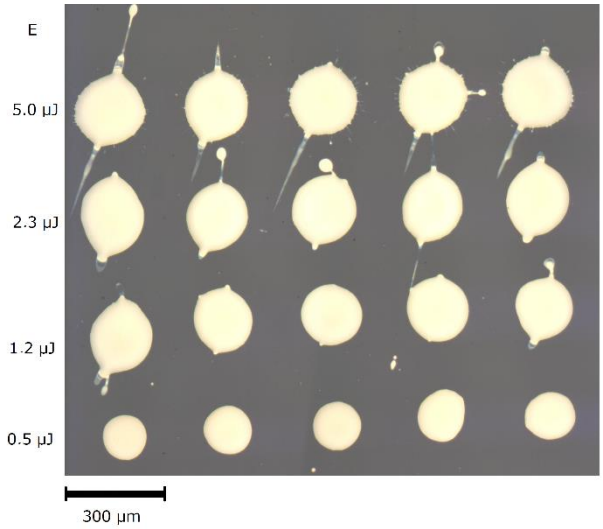

FIG. 2: Images of dried droplets deposited using various laser pulse energies, the average energies of each row are indicated on the left side of the image.

Even though five energies were used only four of them produced droplets. That is because there is a minimum fluence threshold that must be surpassed in order to complete the transfer process [6,9]. Laser energies below 0.2 μJ did not produce the deposition of a droplet.

The droplets have a circular shape and their radius increases with the energy, even though the droplet radius seems to reach a maximum at about 2.3 μJ. Higher energy laser pulses yield more irregular droplet profiles. The most homogenous circular droplet shapes are achieved with an energy of 0.5 μJ; at higher energies splashing is present. As the laser energy increases, also does the kinetic energy of the jet when it collides with the substrate, which could explain the increased splashing at higher laser energies [9]. The most noticeable splashing tends to follow a diagonal pattern. The not symmetrical laser Gaussian profile, discovered while measuring the laser beam diameter in the next section, can explain this fact. At the highest energy, 5 μJ, a particular pattern of splashing is observed. It corresponds to a smaller thread with tiny splashing located around the droplets.

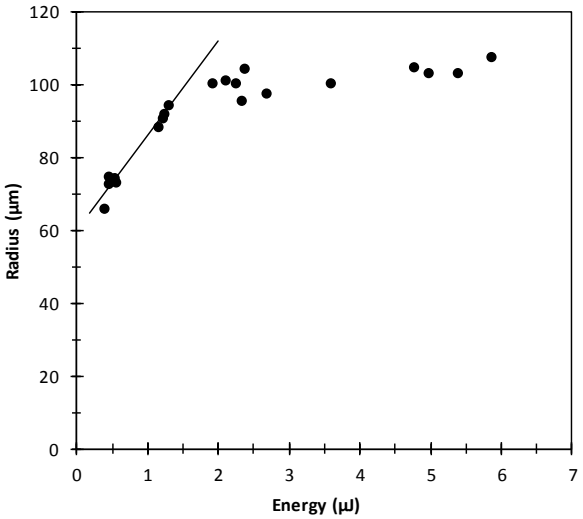

FIG. 3: Plot of the droplet radius versus laser pulse energy.

Fig.3. shows the dependence of the droplet radius with the laser pulse energy. A linear dependence is found at the energy range of 0.5-2 μJ. At higher energies, the dependence changes and the radius seems to approach a maximum value. The maximum droplet radius could be attributed to a depletion of the ink in the area surrounding the irradiated spot at a given energy. Thus, further increase of the energy does not affect the droplet radius and additionally, as seen in Fig.2., produces more splashing.

B. LASER BEAM DIAMETER

A critical parameter involved in the transfer process is the laser beam diameter [6,9]. To study this parameter the experimental setup was not changed but the donor substrate was replaced by a microscope glass coated with a titanium layer. The laser beam was focused on the titanium coating and when the laser fluence was higher than the threshold fluence the titanium was ablated. An array of ablations was obtained. The radius of the titanium ablations was measured using the optical microscope. They had a quasi-elliptical shape, evidencing that the laser was a not perfectly symmetrical Gaussian.

According to the model [6,9] the Gaussian fluence profile of the laser beam is given by the following equation

$$F = \frac{2E}{\pi\omega^2} e^{-\frac{2r^2}{\omega^2}} \qquad (1)$$

where E is the laser pulse energy, ω the laser beam diameter and r the laser beam radius. The titanium is only ablated when the fluence value surpasses the threshold fluence so the fluence at exactly the ablation radius equals to the fluence threshold. Knowing this, it is followed from equation (1) that when plotting the square of the ablation radius vs the laser pulse energy, a linear dependence should be obtained. It is possible to use this fact to obtain the titanium fluence threshold and the laser beam diameter.

The results of the measurement are shown in Fig.4. The linear dependence of the values should be noted. The laser diameter was found to be 11 μm and the threshold fluence for titanium 1.5 J/cm^2. Both are plausible values; the threshold fluence's order of magnitude is the same than that of the fluences used to print with a DRL in [8].

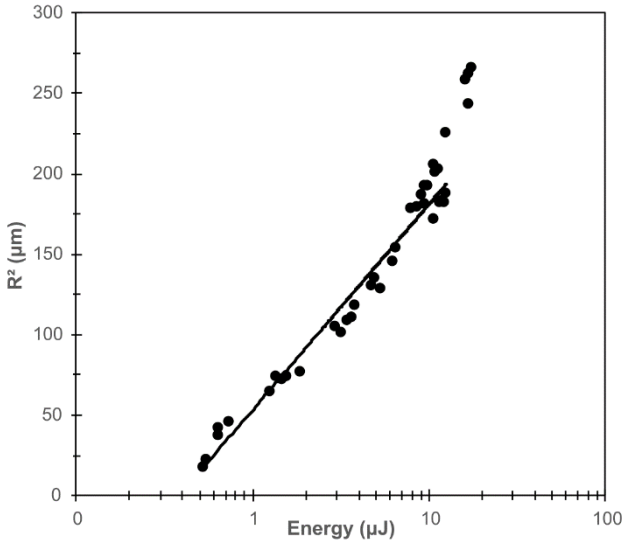

FIG. 4: Plot of the square of the ablation radius vs the laser pulse energy.

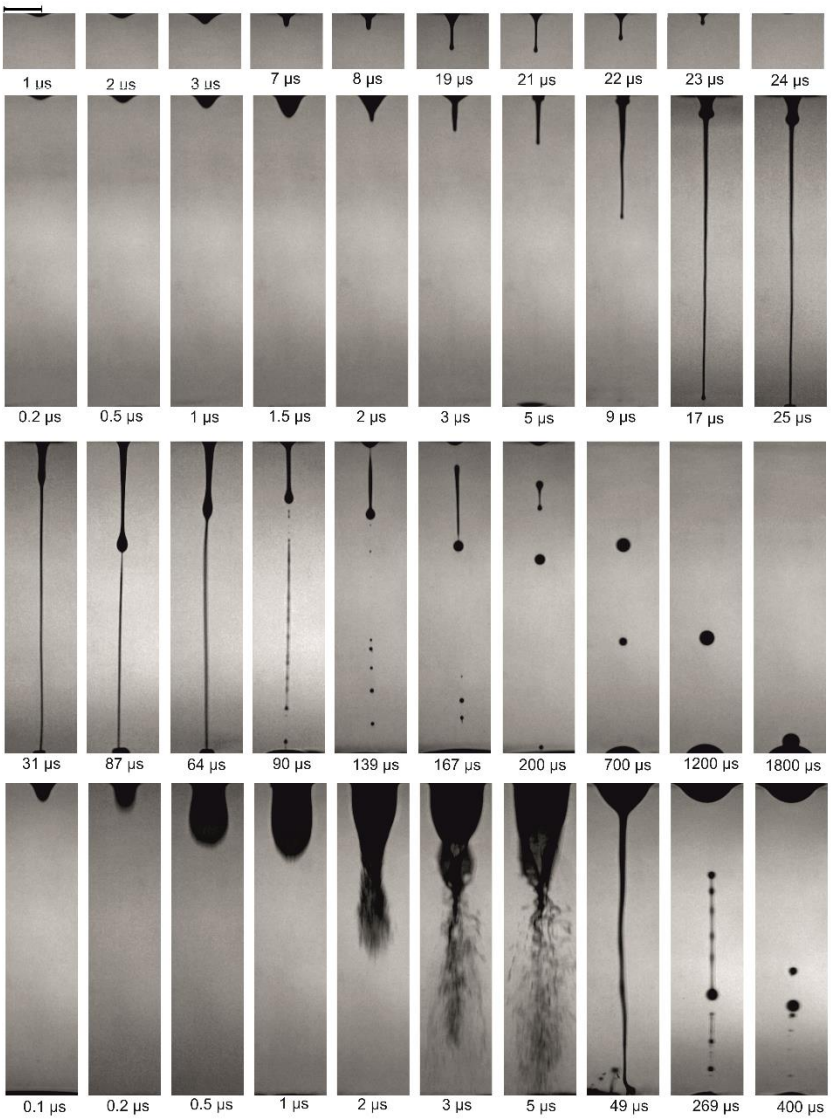

FIG.5: Images of the transfer process, below each image there is the delay respect to the laser pulse. The average laser pulse energy employed in obtainment of first row is 0.13 μJ. For the next two rows of images it is 0.56 μJ and in the last one it is 5.1 μJ. The scale line value is 0.15 mm

C. TRANSFER PROCESS DYNAMICS

Fig.5. shows the transfer process at three values of the laser pulse energy. The donor substrate is located in the upper portion of the image and the acceptor substrate is placed below it, at the bottom edge of the image. Starting with the process at 0.13 μJ, in the initial microseconds a protuberance appears on the liquid film. This protuberance is smaller than those observed for processes at higher energies. A thin jet is formed that begins to move downwards, its advance is stopped at 21 μs when the jet starts to retract. The jet ends up reaching the donor substrate again at 24 μs.

The second and third row illustrate the process at 0.56 μJ. In early times, the first noticeable feature is again the apparition of a protuberance in the homogenous ink layer. The protuberance grows until it reaches a maximum size at 1.5 μs. Then, at 2 μs, a thin spike shaped jet begins to form at the bottom tip of the protuberance. This jet goes downward and reaches the acceptor substrate at 17 μs, where the deposition process begins. A second thicker jet emerges from the ink layer at 5 μs. In contrast with the first jet, this second one has a cylinder like shape. The second jet thins as does the ink union between the first and second jet. A droplet is created at the second jet's tip clearly seen at 87 μs. This moment, there is only a slim ink thread keeping both jets together. The union between the jets breaks somewhere between 87 μs and 90 μs. The second jet's union with the ink layer also thins and breaks between 139 μs and 167 μs. The ink detached from the donor substrate is divided into a droplet, the one seen at 87 μs, and a thread. The thread coalesces and turns into a droplet at 700 μs. Both droplets move towards the acceptor substrate and are deposited on it at 1800 μs.

The fourth row in Fig.5 shows the transfer process at 5.1 μJ. A protuberance is also born from the main ink layer but now it expands at a higher speed with an oval-like shape. At 2 μs the protuberance bursts violently spreading ink all over the camera field of view. This is presumably the source of the satellite droplets seen in Fig.2 around the main ones for energies higher than 0.5 μJ. An ink thread is formed at 49 μs which detaches from the donor substrate at 269 μs. The thread falls on the acceptor substrate and is deposited on it. A protuberance is left at the donor film; it was observed that the protuberance reduced its size over time.

The front position of the jets involved in the transfer processes vs time are plotted in Fig.6. A linear dependence is found between both values and the jets' speeds are calculated. The speed of the jet in the low energy process is 7 m/s. For the medium energy, the speed of the first jet is 53 m/s. For the second jet, the speed is 5 m/s. In the high energy case the calculated speed is 326 m/s. The order of magnitude of the speeds is in accordance with other works [5,7-8].

A detailed explanation of the complete transfer process at intermediate energies is given in [7]. It is necessary to summarize the jet creation dynamics for the laser pulse energy of 0.56 μJ to fully understand the dynamics at higher and lower energies. The laser is absorbed by the donor material and a vapor bubble is created in the film. The protuberance seen during the first microseconds of Fig.5 corresponds to the bubble's expansion. The expansion is quicker towards the film-air interface since the bubble has less material to displace in that direction. This creates a pressure gradient between the bubble's top and bottom that induces a liquid flow around its sides. The flow develops a stagnation point between the bubble and the film-air interface [7]. Two jets are created, one that travels towards the acceptor substrate, seen in Fig.5, and another counterjet that moves upwards traversing the bubble [7]. The bubble is divided in two smaller bubbles and a high-pressure ring is born. This ring gives rise to the second jet [7] observed in Fig.5 medium energy process at the delay time of 9 μs. The fact that the creation of the first and second jets are governed by two distinct dynamics is evidenced by the different speeds obtained from Fig.6 second plot. The downwards advance of the droplets formed at 700 μs occurs at a much slower speed than that of the jets, which is manifested by the wide difference in time between the last images. It can be seen in Fig.5 that no bursting of the jet occurs at this energy and that the droplet is deposited gently on the acceptor substrate. The uniform droplets without satellite splashing of Fig.2 at 0.5 μJ correlate well with this behaviour.

In the low energy process, the pressure gradient of the expanding bubble is not high enough to fully project the jet, which is stopped by the surface tension forces. Surface tension also plays a key role in the recoiling of said jet. The minimum pulse fluence required to successfully deposit a droplet using a considerable donor to acceptor distance depends on the liquid's surface tension. Nevertheless, if the fluence is greater than the threshold fluence but does not allow the jet to reach the acceptor substrate passing through the 1.25 mm gap, deposition could also be achieved with a smaller gap.

The violent expansion of the bubble at 5.1 μJ comes from the sudden and high amount of energy absorbed by the donor film. It is also seen that the jet speed in this process is much higher than that of the two previous ones, which proves the higher kinetic energy involved in the process. This kinetic energy is the source of the splashing observed around the main droplets of Fig 2. High energies are not ideal to obtain droplets with a controlled size.

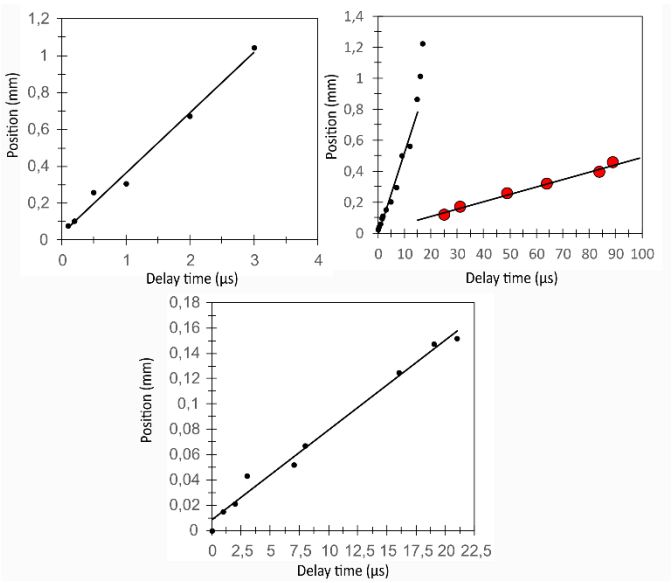

FIG. 6: From left to right and from top to bottom, plots of the front jet position vs the delay time at 0.13 μJ, 0.56 μJ and 5.1 μJ. The second graph contains the evolution of the first jet (black dots) and the second jet (bigger red dots).

IV. CONCLUSIONS

The LIFT transfer process for three different laser pulse energies was examined using a laser beam diameter of 11 μm. For an energy of 0.13 μJ a thin jet was formed but it did not reach the acceptor substrate. For the process at 0.56 μJ two jets were created. Both jets deposited ink gently on the acceptor substrate, the first reaching the acceptor substrate while joined to the donor film and the second one detaching from it and coalescing into droplets. If the energy was too high, 5.1 μJ in the presented experimental conditions, the bursting of the bubble occurred and a non-optimal deposition was obtained. Splashes and satellite droplets appeared around the main ones.

From the images of the droplets and the process dynamics it is concluded that there is a laser pulse energy range for which optimal deposition is obtained. It is located around 0.5 μJ. The existence of a fluence threshold was also proven. However, the minimum fluence required to deposit a droplet is not exactly this threshold fluence, given that there is a range of energies around 0.15 μJ where a jet is created but does not reach the acceptor substrate. Here, the separation between both substrates is an important parameter to take account.

ACKNOLEDGMENTS

I would like to thank my advisor Dr. Pere Serra for his guidance in the completion of this work. Also thanks to Pol Sopeña for his assistance in the laser processing laboratory and to my family and friends for their support, special thanks to Sergio González Torres, Cristian David Quiñonez Faillace and Bernat Rossinyol Tena.

---

[1] Venkata K. R. R., Venkata A., Karthik P.S. and Surya P.S.; Conductive silver inks and their applications in printed and flexible electronics, *RSC Adv*., **5**, 77760-77790, 2015

[2] Calver P.; Inkjet Printing for Materials and Devices, *Chem. Mater.* **13,** 3299-3305, 2001

[3] Craig B. A., Serra P. and Piqué A.; Laser Direct-Write Techniques for Printing of Complex Materials, *MRS Bulletin*, **32**, 23-31, 2007

[4] Delaporte P. and Alloncle A.-P.; Laser-induced forward transfer: A high resolution additive manufacturing techology, *Optics & Laser Technology*, **78,** 33-41, 2015

[5] Boutopoulos C. Kalpyris I. Serpetzoglou E. and Zergioti I. ; Laser-induced forward transfer of siver nanoparticule ink: time-resolved imaging of the jetting dynamics and correlation with the printing quality, *Microfluid Nanofluid*, **16**:493-500, 2013.

[6] Duocastella M., Patrascioiu A., Fernández-Pradas J.M., Morenza J.L. and Serra P.; On the correlation between droplet volume and irradiation conditions in the laser forward transfer of liquids, *Appl Phys A* **109**:5-14, 2012.

[7] Patrascioiu A., Fernández-Pradas J.M., Palla-Papavlu A., Morenza J.L. and Serra P.; Laser-generated liquid microjets: correlation between bubble dynamics and liquid ejection, *Microfluid Nanofluid*, **16**:55-63, 2014.

[8] Duocastella M., Fernández-Pradas J.M., Morenza J.L. and Serra P.; Time-resolved imaging of the laser forward transfer of liquids, J*ournal of applied physics*, **106**, 084907, 2009.

[9] Colina M., Duocastella M., Fernández-Pradas J.M., Serra P. and Morenza J.L.; Laser-induced forward transfer of liquids: Study of the droplet ejection process, *Journal of applied physics*, **99**, 084909 , 2006.